NASA TECHNICAL MEMORANDUM NASA TM X-73592

NASA TM X-73592

(NASA-TM-X-73592) ELASTIC PROPERTIES AND FRACTURE STRENGTH OF QUASI-ISOTROPIC GRAPHITE/EPOXY COMPOSITES (NASA) 16 p HC A02/MF A01 CSCL 11D N77-17164 Unclas G3/24 14891

ELASTIC PROPERTIES AND FRACTURE STRENGTH OF QUASI-ISOTROPIC GRAPHITE/EPOXY COMPOSITES

by T. L. Sullivan
Lewis Research Center
Cleveland, Ohio 44135

TECHNICAL PAPER to be presented at the
Conference on Composites and Advanced Materials
sponsored by the American Ceramic Society
Cocoa Beach, Florida, January 17-19, 1977

E-9060

ELASTIC PROPERTIES AND FRACTURE STRENGTH OF QUASI-ISOTROPIC GRAPHITE/EPOXY COMPOSITES

by T. L. Sullivan

National Aeronautics and Space Administration
Lewis Research Center
Cleveland, Ohio 44135

ABSTRACT

A research program was devised to experimentally determine the properties of four quasi-isotropic laminates. The layups of these laminates were $(0, \pm 60)_s$, $(0, \pm 45, 90)_s$, $(0, \pm 30, \pm 60, 90)_s$ and $(0, \pm 22\ 1/2, \pm 45, \pm 67\ 1/2, 90)_s$. The properties determined were tensile modulus, Poisson's ratio, bending stiffness, fracture strength and fracture strain. Measured properties and properties predicted using laminate theory were found to be in reasonable agreement. Reasons for data scatter were determined.

INTRODUCTION

Laminated fibrous composites are generally thought to be highly directional in character. However, there does exist a genus of laminates that have elastic tensile properties in the plane of the sheet that are the same regardless of the load direction. This type of laminate is generally referred to as a quasi-isotropic laminate (ref. 1). These laminates consist of three or more plys with the angle between each ply constant and equal to (180°/number of plies).

The simplest quasi-isotropic laminate is (0, +60, -60) or in its more commonly used symmetric form (0, +60, -60, -60, +60, 0). This type of laminate can be useful in applications where the load in the plane of the sheet is multidirectional, where the load direction is not known or when the load direction varies with the type of external loading.

This paper describes a research program devised to experimentally determine the elastic properties in tension and bending of quasi-isotropic laminates made from high modulus graphite fiber (Modmor I) and epoxy (ERLA 4617). Four laminate configurations were investigated: $(0, \pm 60)_s$, $(0, \pm 45, 90)_s$, $(0, \pm 30, \pm 60, 90)_s$, and $(0, \pm 22\ 1/2, \pm 45, \pm 67\ 1/2, 90)_s$. These properties are compared to those predicted by laminate theory. In addition, tensile fracture strengths were determined and compared to the strength predicted using a modified distortion energy failure criteria. Finally, reasons are discussed for scatter in the experimental data and the effect of fiber misalignment on predicted elastic tensile properties is examined.

STAR Category 24

EXPERIMENTAL TEST PROGRAM

Laminate Fabrication

The four laminates, each 12 inches square, were supplied by the Research and Development Division of Whittaker Corporation. They were made using high modulus graphite fiber (Modmor I) and epoxy (ERLA 4617). The ply stacking sequences were as follows:

$(0, \pm 60)_s$, $(0, \pm 45, 90)_s$, $(0, \pm 30, \pm 60, 90)_s$, and $(0, \pm 22\ 1/2, \pm 45, \pm 67\ 1/2, 90)_s$.

Each laminate was 12 inches square. Fabrication specifications called for the fiber angle to be within $\pm 1^\circ$ of that specified and the fiber volume ratio to be 0.50 $\pm$0.02.

The cure schedule was as follows:

Room temperature to 250° F at 7 inch Hg vacuum
Hold 40 minutes
Apply 50 psi autoclave pressure
Raise to 350° F
Hold 2 hours
Cool to 120° F or lower under pressure

Specimen Preparation, Instrumentation and Testing

From each of the four laminates, coupon type specimens were cut using a diamond wheel. Each coupon was 0.5 inch wide. The coupon angles referenced to the laminate 0° plies were from 0° to 90° in increments of 15°. One coupon was cut at each angle except for the 0°, 45°, and 90° coupons where two were cut. Figure 1 shows where each coupon was located in the laminate. Coupon lengths ranged from about 6 to 12 inches. The 1-inch wide specimens shown in figure 1 were for determining the notch strengths of the laminates in another program.

After cutting, each coupon had its ends reinforced with 1.5 inch long adhesively bonded fiberglass tabs.

Each coupon was instrumented at its midlength with back-to-back strain gage rosettes. The 0° and 90° coupons were instrumented with 90° tee rosettes while the remaining coupons were instrumented with 60° delta rosettes.

Prior to application of instrumentation, the 0° and 90° coupons were tested in cantilever bending to determine their fundamental frequency. A strobe light was used to measure frequency.

The tensile tests were conducted in a 20 000-pound capacity screw driven universal testing machine (fig. 2). Loading was halted at con-

venient intervals for recording strain gage data.

RESULTS AND DISCUSSION

Bending Moduli

Bending modulus was determined from specimen fundamental bending frequency using the method described in reference 2. These values are tabulated in table I. The predicted values were obtained from a laminate analysis computer code (ref. 3). The experimental values are less than those predicted. The accuracy of the experimental method was verified by determining moduli from load and deflection in 3-point and cantilever bending and comparing these results with the vibration tests. Table I shows the bend test results agreed very well with the vibration results. One explanation for the difference between measured and predicted values may be that the ply has a lower modulus in compression than in tension. The laminate analysis used the ply modulus obtained from a tension test.

While quasi-isotropic laminates should exhibit isotropy in tensile tests, these results show they can be highly anisotropic in bending. However, bending anisotropy can be reduced by selecting another ply stacking sequence. For instance the 12-ply quasi-isotropic laminate $(0, \pm 60, \mp 60, 0)_s$ will show less anisotropy in bending than any of the laminates studied in the present investigation because of the averaging effect obtained from the location of the 0° plies.

Tensile Moduli and Poisson's Ratios

All the experimentally determined tensile moduli and Poisson's ratios are plotted in figure 3. Each data point is an average obtained from the back-to-back strain gages. The strain gage data were reduced using a computer code (ref. 4). Elastic constants were determined using a least squares best fit to the strain gage data.

As can be seen, there was substantial scatter in the data. It appears that the moduli values for the $(0, \pm 30, \pm 60, 90)_s$ laminate lie slightly above those of the other three laminates. It is suspected (but not yet verified) that this laminate had a greater fiber volume content than the others.

Laminate theory prediction of modulus and Poisson's ratio are shown in figure 3. These values were obtained assuming a fiber volume ratio of 0.5 and the ply properties listed in table II. An average of all the data agrees quite well with the theoretical prediction. The average modulus was 11.5×10^6 psi compared to the predicted 11.8×10^6 psi. The average Poisson's ratio was 0.33 compared to the predicted 0.31.

Because of the data scatter and the sometimes large difference in results obtained from the back-to-back strain gages, some of the failed

specimens were sectioned for microscopic studies. In some cases it was found that the ply layup was greatly different from that specified. The worst case observed for variation in results from the back-to-back strain gages was one of the coupons from the $(0,\pm30, \pm60, 90)_s$ laminate loaded at 90°. The stress-strain curves for this coupon are shown in figure 4. A section through the strain gages showed that one of the -30° plies was either wholely missing, partly missing, or greatly misaligned. A photomicrograph of this section is shown in figure 5. For purposes of analysis with laminate theory, this anomaly was estimated to be equivalent to a -30° ply half the thickness of the other plies. Using this estimation, laminate theory predicted slopes very close to those obtained experimentally as shown in figure 4. The value of using back-to-back strain gages for obtaining stress-strain curves was clearly demonstrated. The bending-streching coupling that takes place in nonsymmetric laminates was clearly illustrated.

Because of the obvious misalignment of some of the plies as determined in the microscopic studies, laminate theory was used to determine how sensitive the elastic properties under study were to relatively small errors in fiber alignment. The 0° plies were the ones chosen to be perturbed up to 5°. Both plies were perturbed the same amount in order to maintain symmetry about the laminate midplane. Figure 6 shows the effect of 1°, 3°, and 5° misalignments on tensile modulus for the $(0, \pm60)_s$ laminate. For a misalignment of 5° and a load angle of about 25°, the predicted tensile modulus is 11.5 percent less than that of the truly quasi-isotropic laminate. Figure 7 shows the effect of 5° misalignment on the tensile modulus of the other laminates. The misalignment of two plies has a diminishing effect as the total number of plies in the laminate increases.

Figure 8 shows the effect of misalignment on Poisson's ratio for the $(0, \pm60)_s$ laminate. For a misalignment of 5° and a load angle of about 60°, the predicted Poisson's ratio is 18 percent less than that of the truly quasi-isotropic laminate. Figure 9 shows the effect of a 5° misalignment on Poisson's ratio of the other laminates. These studies indicate that Poisson' ratio is more sensitive to fiber misalignment than is tensile modulus. If fiber misalignment were the cause of the data scatter, then one would expect greater scatter in Poisson's ratio data. And this is indeed the case. Table III lists the mean, standard deviation, and coefficient of variation $\left(\frac{\text{standard deviation}}{\text{mean}}\right)$ for each laminate. Except for the $(0,\pm60)_s$, laminate, the coefficient of variation for the Poisson's ratios is substantially greater than for tensile modulus.

Fracture Strengths

While theory predicts isotropic in-plane elastic properties for the laminates under study, the same is not true for fracture strengths. A modified distortion energy criteria available in the computer code previously referred to was used to predict failure. This criteria

predicted first failure by transply cracking induced by residual stress alone. However, this would not cause total laminate failure. If this mode of failure is removed from the analysis, predicted strength for the $(0, \pm 60)_s$ laminate would be as shown in figure 10. This laminate was chosen because as the number of ply orientations increase, strength approaches the minimum value shown in figure 10. Here total laminate failure is induced by ply longitudinal tensile fracture. While transply cracking would not cause laminate failure, it could weaken the laminate by reducing its shear strength. Predicted laminate strength for reductions in shear strength of 40 and 60 percent are shown in figure 10. The measured data are included for comparison and are in reasonably good agreement with the reduced shear strength predictions.

With reduced shear strength, the predicted mode of failure changes for 30° and 90° coupons from a tensile failure to a shear failure. Figure 11 shows scanning electron microscope (SEM) photo-micrographs of the fracture surfaces of a 0° and 90° coupon. There is an obvious difference in the fracture surfaces indicative of different failure modes.

All the experimentally determined fracture strengths and strains are plotted in figure 12. As with the elastic property data, the fracture strengths exhibit considerable scatter. The $(0, \pm 30, \pm 60, 90)_s$ laminate fracture strengths in general fall above the remaining data. Similar behavior was noted for tensile modulus values obtained from this laminate.

One explanation for the scatter in fracture strength is a variation from coupon to coupon in the error in fiber direction and fiber volume ratio. Tensile modulus should be affected by these factors in a similar manner. Therefore, if these two factors are contributing to scatter, fracture strain should exhibit less scatter. As can be seen in figure 12, there is less scatter in fracture strain. The scatter is about two-thirds that of fracture strength.

SUMMARY OF RESULTS

An investigation of elastic properties and strength of four quasi-isotropic laminates was conducted. The major results of this investigation were:

1. The average tensile modulus and Poisson's ratio obtained from tensile tests were in good agreement with those predicted by theory. However, the data scatter was quite large.

2. Laminate theory showed that tensile modulus and Poisson's ratio of quasi-isotropic laminates were quite sensitive to fiber misalignment. The evidence strongly suggests that fiber misalignment combined with variation in fiber volume content is responsible for

the data scatter in the elastic constants as well as fracture strength.

3. For the (0, ±60)s laminate, measured and predicted strengths were in reasonable agreement if the ply shear strength was reduced to account for damage caused by residual stress.

4. The value of using back-to-back strain gages on angle plied composites in order to avoid misleading results was clearly demonstrated.

REFERENCES

1. R. M. Jones, Mechanics of Composite Materials. Scripta Book Co., Washington, D.C., 1975.

2. C. C. Chamis, J. H. Sinclair, and T. L. Sullivan, "NASTRAN as an Analytical Research Tool for Composite Mechanics and Composite Structures," Proceedings of the Fifth NASTRAN Colloquium, NASA TM X-3428, 1976, pp. 381-417.

3. C. C. Chamis, "Computer Code for the Analysis of Multilayered Fiber Composites - Users Manual," NASA TN D-7013, Mar. 1971.

4. C. C. Chamis, J. F. Kring, and T. L. Sullivan, "Automated Testing Data Reduction Program," NASA TM X-68050, 1972.

TABLE I. - PREDICTED AND MEASURED BENDING STIFFNESS OF QUASI-ISOTROPIC LAMINATES

Laminate layup	Load direction, deg	Bending stiffness, 10^6 psi			
		Predicted	Measured		
			Vibration	Three-point bending	Cantilever bending
$[0, \pm 60]_s$	0	23.4	20.0 22.4	20.2	16.9
	90	6.3	3.4 3.4	5.1	3.2
$[0, \pm 45, 90]_s$	0	20.4	15.9 16.9	14.7	15.8
	90	4.4	3.4 3.4	3.3	3.0
$[0, \pm 30, \pm 60, 90]_s$	0	20.0	16.9 18.2	17.3	[illegible]
	90	3.9	2.9 3.1	2.8	2.9
$[0, \pm 22\frac{1}{2}, \pm 45, \pm 67\frac{1}{2}, 90]_s$	0	20.1	16.6 16.7	12.7	18.1
	90	3.7	2.7 2.8	2.6	2.8

TABLE II. - PLY PROPERTIES USED IN LAMINATE ANALYSIS[a]

Longitudinal tensile modulus, psi	32.6×10^{6}
Transverse tensile modulus, psi	1.1×10^{6}
Shear modulus, psi	0.71×10^{6}
Poisson's ratio	0.184
Longitudinal thermal coefficient of expansion, in/in/°F	-0.5×10^{-6}
Transverse thermal coefficient of expansion, in/in/°F	26×10^{-6}
Longitudinal tensile strength, psi	78 000
Longitudinal compressive strength, psi	66 200
Transverse tensile strength, psi	5 820
Transverse compressive strength, psi	29 000
Shear strength, psi	6 520

[a]Provided by fabricator.

TABLE III. - MEAN VALUES, STANDARD DEVIATIONS AND COEFFICIENTS OF VARIATION FOR

ELASTIC CONSTANTS OF QUASI-ISOTROPIC LAMINATES

Laminate layup	Tensile modulus			Poisson's ratio		
	Mean, 10^6 psi	Standard deviation, $X10^{-6}$	Coefficient of variation, percent	Mean	Standard deviation	Coefficient of variation, percent
$[0, \pm 60]_s$	11.5	0.893	7.77	0.323	0.0250	7.74
$[0, \pm 45, 90]_s$	11.0	.787	7.15	.316	.0530	16.78
$[0, \pm 30, \pm 60, 90]_s$	12.3	.712	5.79	.335	.0364	10.87
$[0, \pm 22\frac{1}{2}, \pm 45, \pm 67\frac{1}{2}, 90]_s$	10.9	.699	6.41	.327	.0422	12.92

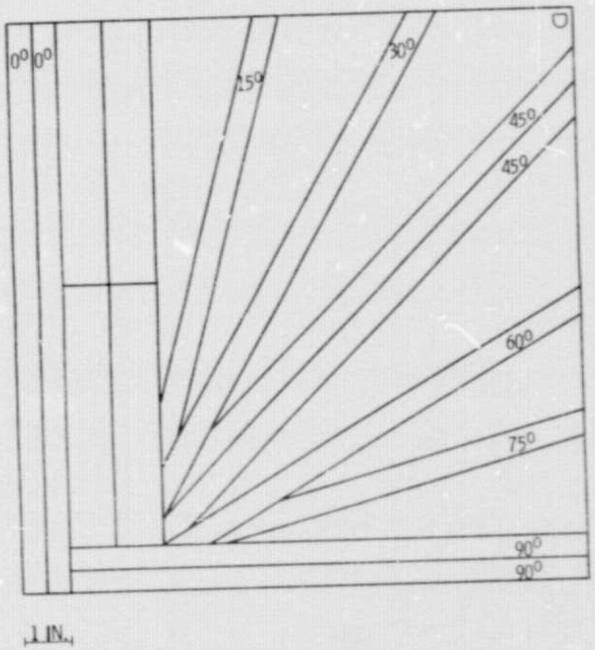

Figure 1. - Specimen layout.

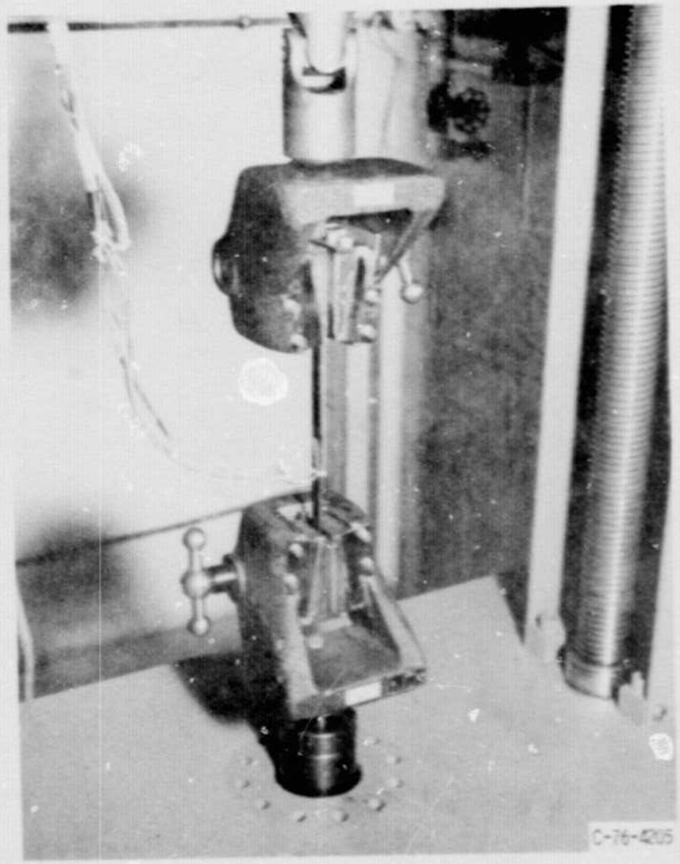

Figure 2. - Tensile test apparatus.

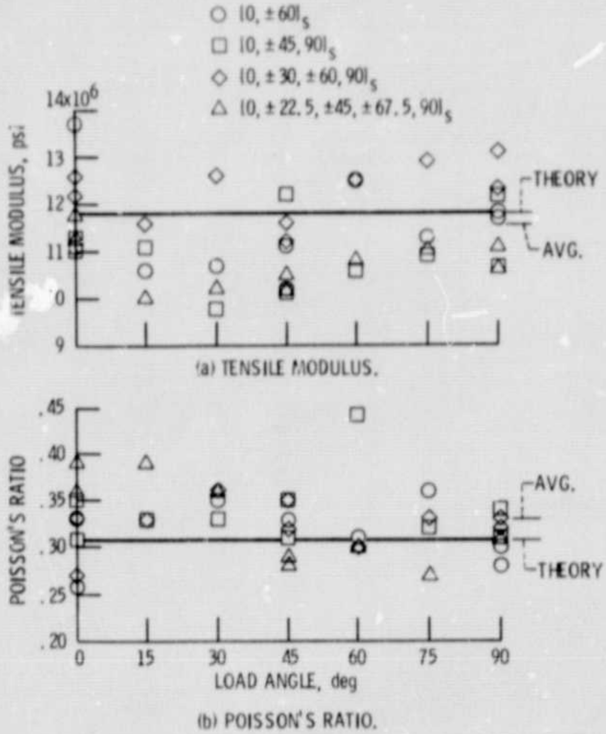

Figure 3. - Elastic properties of quasi-isotropic laminates.

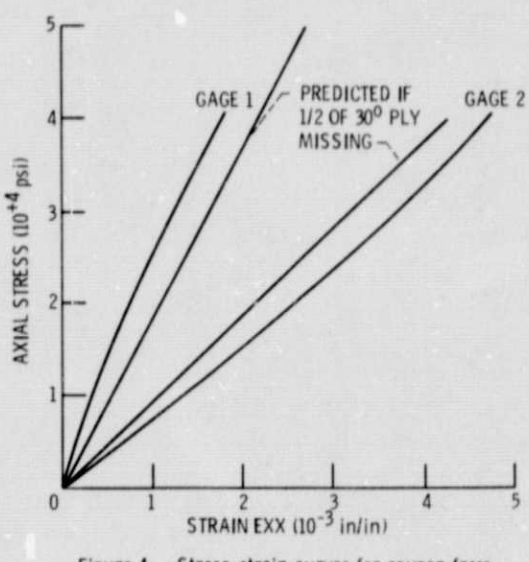

Figure 4. - Stress-strain curves for coupon from [0, ± 30, ± 60, 90]s, laminate tested at 90°.

E-9060

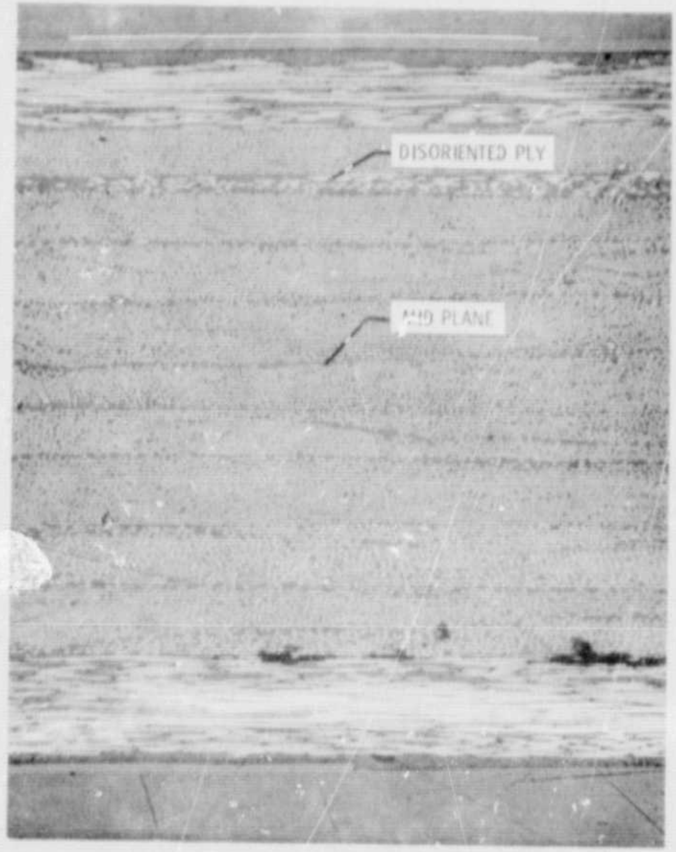

Figure 5. - Photomicrograph of section through $[0, +30, +60, 90]_s$ laminate.

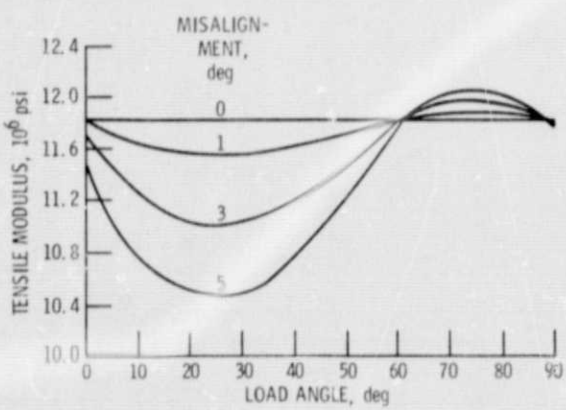

Figure 6. - Effect of misalignment of 0^o plies on $[0, \pm 60]_s$ laminate tensile modulus.

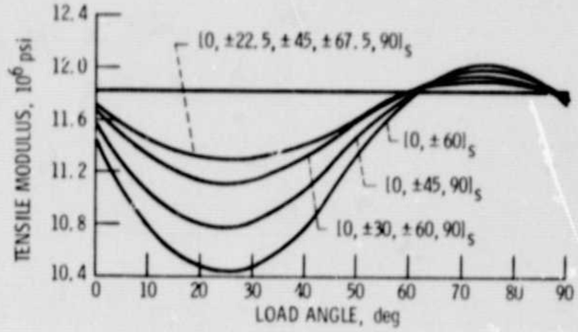

Figure 7. - Effect of 5^0 misalignment of 0^0 plies on the tensile modulus of four laminates.

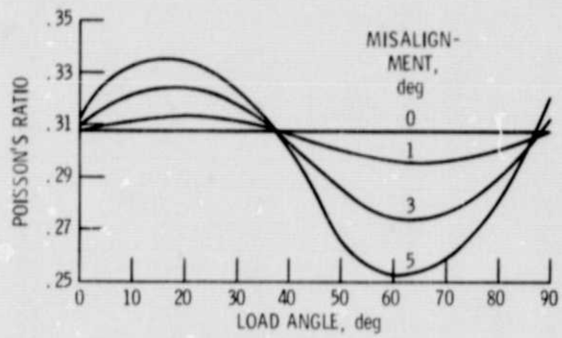

Figure 8. - Effect of misalignment of 0^0 plies on [0, ±60]$_s$ laminate Poisson's ratio.

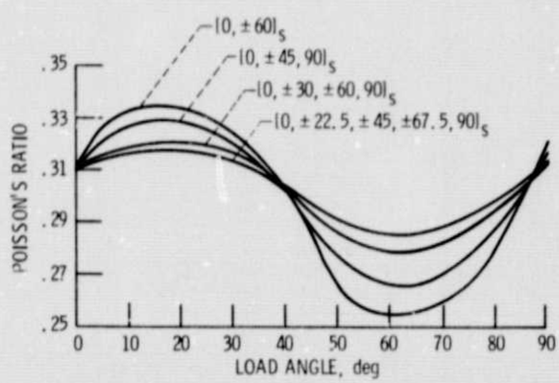

Figure 9. - Effect of 5^0 misalignment of 0^0 plies on the Poisson's ratio of four laminates.

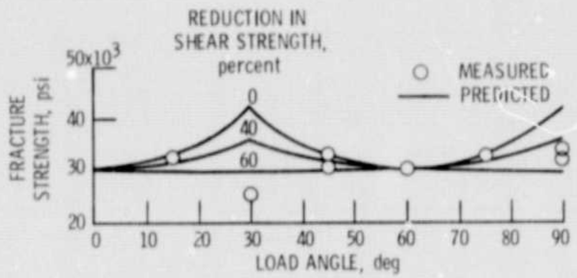

Figure 10. - Comparison of predicted and measured strength for $[0, \pm 60]_s$ laminate.

E-9060

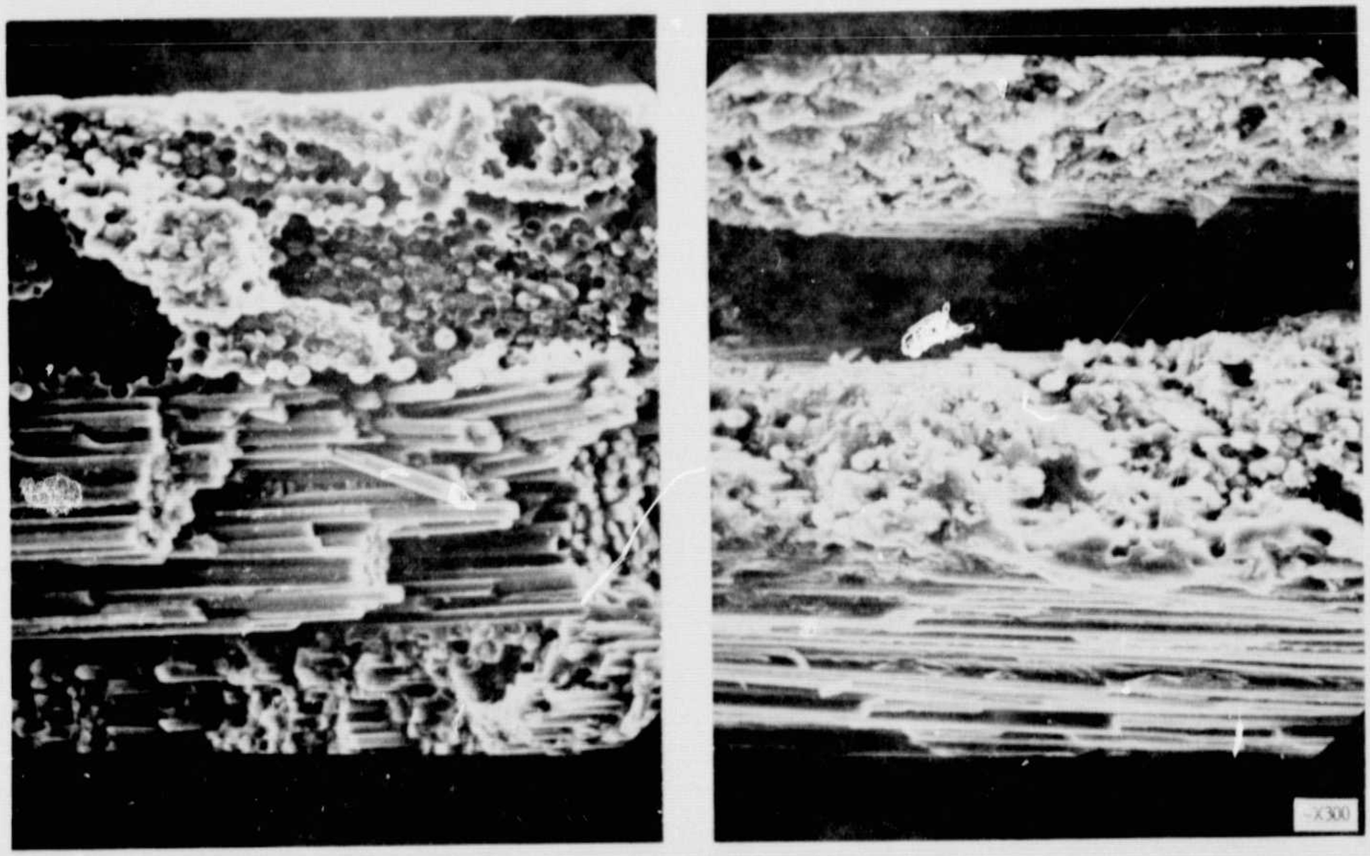

(a) 0^{0} LOAD DIRECTION

(b) 90^{0} LOAD DIRECTION

Figure 11. - Scanning electron microscope photomicrographs of fracture surfaces from $[0, +60]_s$ laminate.

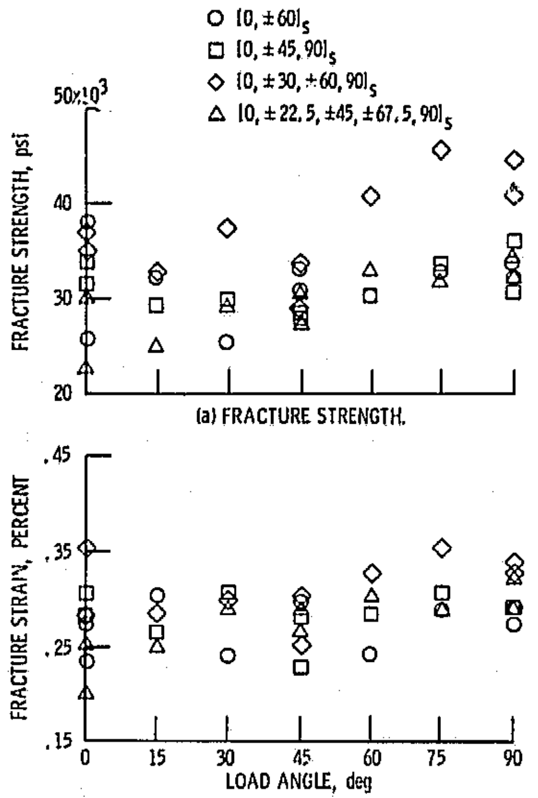

(b) FRACTURE STRAIN.

Figure 12. - Fracture properties of quasi-isotropic laminates.